

# Distinct Responses to Mechanical Grinding and Hydrostatic Pressure in Luminescent Chromism of Tetrathiazolyothiophene

Kazuhiko Nagura,<sup>†</sup> Shohei Saito,<sup>\*,†,‡</sup> Hitoshi Yusa,<sup>||</sup> Hiroshi Yamawaki,<sup>⊥</sup> Hiroshi Fujihisa,<sup>⊥</sup> Hiroyasu Sato,<sup>#</sup> Yuichi Shimoikeda,<sup>∇</sup> and Shigehiro Yamaguchi<sup>\*,†,§</sup>

<sup>†</sup>Department of Chemistry, Graduate School of Science, and <sup>§</sup>Institute of Transformative Bio-Molecules (WPI-ITbM), Nagoya University, Furo, Chikusa, Nagoya 464-8602, Japan

<sup>‡</sup>PRESTO, Japan Science and Technology Agency (JST), Furo, Chikusa, Nagoya 464-8602, Japan

<sup>||</sup>National Institute for Materials Science, 1-1 Namiki, Tsukuba, Ibaraki 305-0044, Japan

<sup>⊥</sup>National Institute of Advanced Industrial Science and Technology, 1-1-1 Higashi, Tsukuba, Ibaraki 305-8565, Japan

<sup>#</sup>Rigaku Corporation, 3-9-12 Matsubara, Akishima, Tokyo 196-8666, Japan

<sup>∇</sup>JEOL Resonance Inc., 3-1-2 Musashino, Akishima, Tokyo, 196-8558, Japan

## Supporting Information

**ABSTRACT:** Luminescent mechanochromism has been intensively studied in the past few years. However, the difference in the anisotropic grinding and the isotropic compression is not clearly distinguished in many cases, in spite of the importance of this discrimination for the application of such mechanochromic materials. We now report the distinct luminescent responses of a new organic fluorophore, tetrathiazolyothiophene, to these stresses. The multichromism is achieved over the entire visible region using the single fluorophore. The different mechanisms of a blue shift by grinding crystals and of a red shift under hydrostatic pressure are fully investigated, which includes a high-pressure single-crystal X-ray diffraction analysis. The anisotropic and isotropic modes of mechanical loading suppress and enhance the excimer formation, respectively, in the 3D hydrogen-bond network.

Mechanochromic luminescent molecules have recently attracted attention due to their great potential for various applications, such as memory devices and sensors.<sup>1</sup> A number of mechanochromic systems based on organic molecules,<sup>2</sup> metal complexes,<sup>3</sup> and polymers have been rapidly developed.<sup>4</sup> In these reports, the molecular orientation and intermolecular interactions are perturbed by mechanical forces, viz., shearing, grinding, tension, or hydrostatic pressure, to undergo a drastic emission color change. However, there are only a few reports that describe the responses to both the mechanical grinding and hydrostatic pressure,<sup>5</sup> despite the importance of these factors when considering the applications of these materials. Since the molecular systems that show distinct spectral responses to these stresses are rather scarce, the difference between the anisotropic grinding and the isotropic compression has not been clearly discriminated. Here, we report the distinct luminescent responses to these stresses using a new fluorophore, tetrathiazolyothiophene **1** (Figure 1). The origin of this difference has been experimentally and theoretically elucidated in detail. The

results demonstrate the importance to discriminate these mechanical stresses.

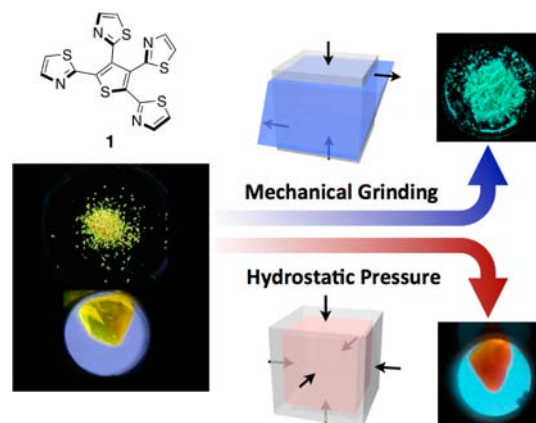


**Figure 1.** Tetrathiazolyothiophene **1** and its yellow-emissive crystals (left) and distinct luminescent responses to mechanical grinding, producing a green-emissive powder, and to hydrostatic pressure, affording an orange-emissive crystal (right).

2,3,4,5-Tetra(2-thiazolyl)thiophene **1** was readily synthesized in 71% yield by the Kosugi–Migita–Stille coupling of tetrabromothiophene with 2-stannylthiazole in refluxing *m*-xylene (Scheme S1). A single-crystal X-ray diffraction (XRD) analysis revealed the molecular structure of **1** (Figure 2). In the crystal structure, the thiazole rings **A** and **D** take almost coplanar arrangements with the central thiophene ring with the dihedral angles of 18.5 and 3.0°, respectively, indicative of an effective  $\pi$ -conjugation in the 2,5-dithiazolyothiophene skeleton. On the other hand, the thiazole rings **B** and **C** adopt twisted conformations with the large dihedral angles of 69.0 and 78.6°, respectively. The high planarity of the 2,5-dithiazolyothiophene skeleton may be partly due to short intramolecular N...S

Received: June 3, 2013

Published: July 1, 2013

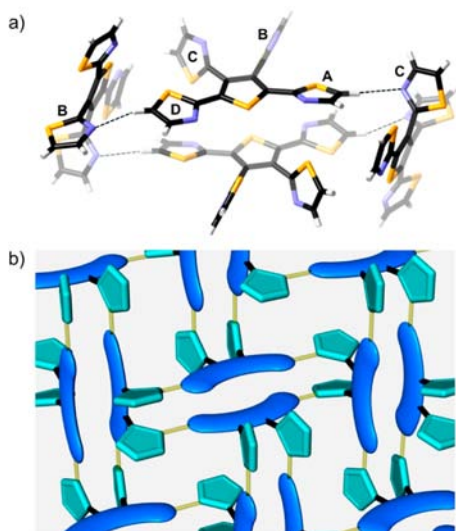


**Figure 2.** Crystal packing structure of **1**: (a) face-to-face dimer fixed with weak C–H...N hydrogen bonds (dotted line) and (b) representation of the crystal packing. Blue boards, green pentagons, and yellow cylinders demonstrate teraryl fluorophores, twisted thiazole rings B and C, and C–H...N hydrogen bonds between the thiazole rings, respectively.

contacts<sup>6</sup> (3.03 and 3.00 Å), which are much shorter than the sum of the van der Waals radii of the N and S atoms (3.35 Å). The single point DFT calculation using the crystal structure showed that its HOMO and LUMO are mainly delocalized on the planar 2,5-dithiazolylthiophene moiety, supporting its effective  $\pi$ -conjugation (Figure S25).

In a CH<sub>2</sub>Cl<sub>2</sub> solution, while compound **1** showed a broad absorption band with the maximum at 373 nm, a sky-blue fluorescence was observed with the maximum wavelength ( $\lambda_{em}$ ) of 453 nm.<sup>7</sup> In contrast, the crystals of **1** exhibited a yellow emission with the  $\lambda_{em}$  of 556 nm. By grinding the crystals, the emission color was largely blue-shifted to green ( $\lambda_{em}$  = 490 nm) with a slight enhancement of the quantum yield ( $\Phi_F$ ) from 0.02 to 0.05. The energy difference in  $\lambda_{em}$  between before and after grinding the crystals amounts to 2420 cm<sup>-1</sup>. The initial yellow emissive state was reproduced by recrystallization of the ground sample.<sup>8</sup> Moreover, **1** showed a blue emission ( $\lambda_{em}$  = 449 nm) in a polymethyl methacrylate (PMMA) film (10 wt % of **1**). These results demonstrated the uniqueness of **1** as a fluorophore that can exhibit the tricolor emissions only by changing the solid environments (Figure 3).

The crystal packing structure of **1** gave insights into the origins of the long-wavelength emission in the crystalline state and its mechanochromism. This compound forms weak intermolecular C–H...N hydrogen bonds at several positions (Figure S14). A relatively strong interaction was observed between the H atoms at the 5-position of the D or A ring and the N atom of the B or C ring in the adjacent molecules (Figure 2a). The hydrogen bonds play an important role in fixing the orientation of the two  $\pi$ -conjugated 2,5-dithiazolylthiophene skeletons in a face-to-face fashion. The distance between the mean planes of the planar teraryl skeletons (3.96 Å) is longer than those of typical  $\pi$ -stacked structures (3.4–3.7 Å), indicating that the teraryl  $\pi$ -skeletons are arranged slightly apart from each other, rather than being closely packed. These multiple intermolecular hydrogen bonds construct a 3D hydrogen-bond network in which the face-to-face teraryl

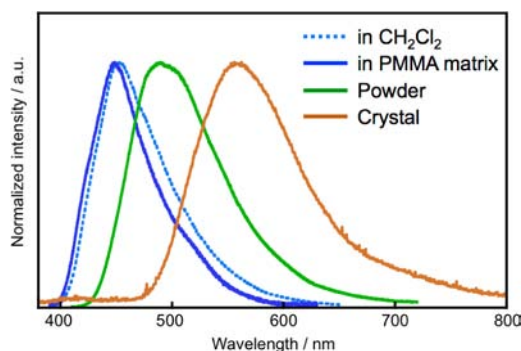


**Figure 3.** Fluorescence spectra of **1** in a CH<sub>2</sub>Cl<sub>2</sub> solution (dotted line), in a PMMA film with 10 wt % of the sample (blue), in a ground powder (green) and in the crystalline state (dark yellow).

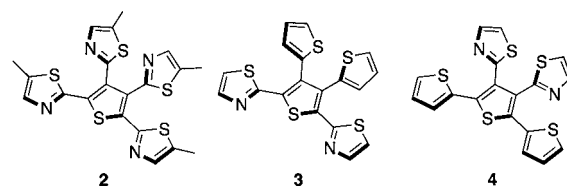
dimers are integrated (Figure 2b). This crystal structure should give rise to the intermolecular interaction of the teraryl skeletons in the ground state. Indeed, **1** showed a red-shifted absorption band in the diffuse reflectance spectrum of the crystalline and powder samples compared to that of the PMMA film (Figure S12).

This structural analysis suggests that the broad and structureless spectrum of the yellow emission band in the crystalline state is attributed to the preformed excimer.<sup>9</sup> This is consistent with the slightly longer fluorescence lifetime of the yellow emission in the crystalline state (0.42 ns) compared to those of the green emission in the ground powder (0.32 ns) and the blue emission in solution (0.14 ns).

Upon grinding the crystals, the weak 3D hydrogen-bond network is disordered without forming another long-range ordered phase. In the powder XRD measurements of **1**, the diffraction peaks of the crystalline sample became gradually broadened, while in turn, a broad halo band increased in intensity when the sample was ground for a long time (Figure S15). The solid-state <sup>1</sup>H NMR spectrum of the ground powder **1** also showed broadened peaks compared to those of the crystalline sample (Figure S17). The comparison in the second derivative curves of the IR spectra before and after grinding the crystals suggested that the degree of the intermolecular hydrogen bonds was perturbed (Figure S16). In conjunction with this change, the face-to-face dimeric structure is likely deformed into a nonordered structure. As a consequence, the yellow-emissive excimer is no longer formed. Instead, the degree of the intermolecular distances between the neighboring fluorophores varies to some extent, resulting in a broad fluorescence band with a green color.<sup>10</sup>

This remarkable response to mechanical grinding is unique to the tetrathiazolyl-substituted compound **1**. The analogous compounds shown in Chart 1, including the tetramethylated 2,3,4-dithienyl **3**, and 2,5-dithienyl **4**, constructed neither the 3D hydrogen-bond network nor the face-to-face dimeric structures in their crystal packings (Figures S2–S7). As a result, the

#### Chart 1. Chemical Structures of Reference Compounds 2–4



structured emission bands were observed for 2–4 with the  $\lambda_{\text{em}}$  of 521, 516, and 525 nm in the crystalline state, respectively, while all these compounds have a  $\lambda_{\text{em}}$  around 455–465 nm in a  $\text{CH}_2\text{Cl}_2$  solution and in a PMMA film (Figures S9–S11). The extent of the red shifts from the solution or the PMMA matrix to the crystalline state for these compounds is smaller than that for 1.<sup>11</sup> In addition, the green emission colors of 2–4 in the crystalline state were not significantly changed between before and after grinding (Figures S9–S11).

On the other hand, compound 1 showed a significant red shift in the fluorescence maximum under hydrostatic pressure (Figure 4). The high-pressure experiments were performed

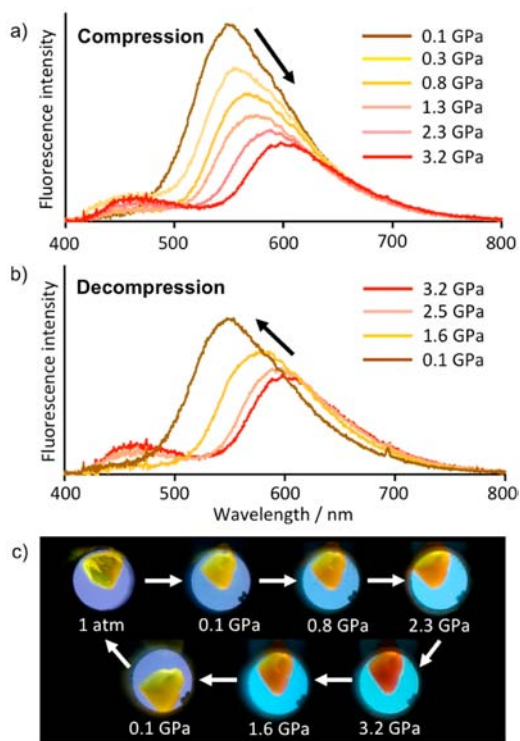


**Figure 4.** Fluorescence microspectroscopy of 1 (crystal) under high pressure: (a) compression and (b) decompression processes in the range of 0.1–3.2 GPa. (c) Micrographs of the crystal under high pressure. A UV LED lamp was used for the excitation ( $\lambda_{\text{ex}} = 365$  nm).

using a diamond anvil cell (DAC). Hydrostatic pressure was applied up to 3.2 GPa in the medium of a 16:3:1 methanol/ethanol/water mixed solvent. During the compression process, the fluorescence maximum was gradually red-shifted from 556 nm, and the intensity concomitantly decreased in response to the external pressure. Eventually, 1 showed an orange fluorescence at 3.2 GPa with a strong emission band at 609 nm.<sup>12</sup> The energy difference in the red shift amounts to 1570  $\text{cm}^{-1}$ . Notably, when the hydrostatic pressure was gradually returned to ambient pressure, the fluorescence spectra turned back to the original emission band at 556 nm. This reversible pressure dependence in the luminescence is worthy of note in the chemistry of mechanochromism, although some polymers have been reported to show a reversible response in their absorption properties.<sup>13</sup>

The high-pressure IR spectra of 1 up to 3.2 GPa revealed the reversible deformation of its hydrogen-bond network (Figure S19). All the stretching vibration modes of the relevant C–H bonds were successfully assigned based on the simulated

spectra under high-pressure conditions. The continuous change in the IR spectra with an increase in pressure implies that no significant phase transition occurs up to the applied pressure of 3.2 GPa. The lower-frequency IR absorption band at 3061  $\text{cm}^{-1}$  at ambient pressure was assigned to the C–H stretching mode of the relatively strong hydrogen bond between the thiazole rings A and C. This band was shifted to the lower frequency of 3035  $\text{cm}^{-1}$  at 3.2 GPa, whereas the other bands were shifted to higher frequencies under high pressure. The decreased frequency suggests the strengthening of the corresponding hydrogen bond, which is consistent with the closer distance and more straight arrangement of the C–H...N geometry in the optimized packing structure under high pressure calculated by the DFT method with the GGA-PBE functional (Figures S20, S24 and Table S7). By releasing the applied pressure, the IR spectrum was restored to the initial one.

A high-pressure single-crystal XRD analysis of 1 using a DAC (up to 2.8 GPa, Figure 5)<sup>14</sup> and the optimized geometries

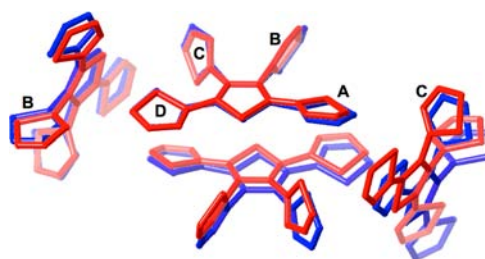


**Figure 5.** Superimposed view of the X-ray crystal packing structures of 1 at ambient pressure (blue) and at 2.8 GPa (red).

under high pressure (up to 4.0 GPa, Figure S23) showed similar compression behaviors in the packing structure to each other. The hydrogen-bonded lattice is deformed, which reduces the void space between the face-to-face 2,5-dithiazolythiophene moieties. The interfacial distance between their mean planes becomes much shorter from 3.96 Å at the ambient pressure to 3.69 Å at 2.8 GPa, according to the X-ray crystallographic analysis. In addition, the two teraryl skeletons have slipped along the long axis, so that these units overlap with each other to a greater extent. The DFT calculation of the closely stacked dimer in the optimized geometry indicated the greater orbital interaction between the two teraryl units at 3.0 GPa than that at ambient pressure (Figure S26). As a result of the closer proximity, a highly overlapped excimer is formed, which is likely the origin of the red-shifted emission under hydrostatic pressure.

In summary, we demonstrate the distinct luminescent responses of a tetrathiazolythiophene fluorophore to anisotropic grinding and isotropic compression. The excimer formation in the 3D hydrogen-bond network is responsible for the yellow emission at 556 nm in the crystalline state. Grinding of the crystals leads to an increase in the disordered phase in which the excimer formation is suppressed and thereby a blue-shifted green-color emission emerges with the  $\lambda_{\text{em}}$  at 490 nm in the powder state. In stark contrast, the high-pressure experiments using a DAC demonstrated that the yellow-excimer emission of the crystals is changed to an orange fluorescence with the  $\lambda_{\text{em}}$  at 609 nm at 3.2 GPa. A high-pressure single-crystal XRD analysis unambiguously determined the closer arrangement of the face-to-face dimer of the fluorophore, which is the origin of the more red-shifted excimer emission.

The reversible structural deformation of the hydrogen-bond network upon compression/decompression is confirmed from both experimental and theoretical studies. Notably, this fluorophore exhibits a blue emission at 449 nm in the PMMA film. Thus, the multichromism covering the entire visible region from blue to orange is achieved using the single fluorophore only by changing the solid state and the types of the mechanical forces. The discrimination between an anisotropic stress by mechanical grinding and an isotropic stress by hydrostatic pressure would accelerate and enrich the chemistry of the mechanochromism.

## ■ ASSOCIATED CONTENT

### Supporting Information

Experimental procedures, structures, and calculations. This material is available free of charge via the Internet at <http://pubs.acs.org>.

## ■ AUTHOR INFORMATION

### Corresponding Author

s\_saito@chem.nagoya-u.ac.jp; yamaguchi@chem.nagoya-u.ac.jp

### Notes

The authors declare no competing financial interest.

## ■ ACKNOWLEDGMENTS

Work was supported by JST-PRESTO “Molecular technology and creation of new functions” to S.S and JST-CREST “Development of high-performance nanostructures for process integration” to S.Y. K.N. thanks the JSPS Research Fellowship for Young Scientists. We thank Dr. Hirofumi Yoshikawa and Prof. Kunio Awaga (Nagoya University) in the diffuse reflectance measurements and Tatsuo Hikage (High Intensity X-ray Diffraction Laboratory, Nagoya University) in the powder XRD measurements.

## ■ REFERENCES

- (1) Luminescent mechanochromism: (a) Sagara, Y.; Kato, T. *Nat. Chem.* **2009**, *1*, 605. (b) Balch, A. L. *Angew. Chem., Int. Ed.* **2009**, *48*, 2641. (c) Chi, Z.; Zhang, X.; Xu, B.; Zhou, X.; Ma, C.; Zhang, Y.; Liu, S.; Xu, J. *Chem. Soc. Rev.* **2012**, *41*, 3878.
- (2) (a) Sagara, Y.; Mutai, T.; Yoshikawa, I.; Araki, K. *J. Am. Chem. Soc.* **2007**, *129*, 1520. (b) Yoon, S.-J.; Chung, J. W.; Gierschner, J.; Kim, K. S.; Choi, M.-G.; Kim, D.; Park, S. Y. *J. Am. Chem. Soc.* **2010**, *132*, 13675. (c) Zhang, G.; Lu, J.; Sabat, M.; Fraser, C. *J. Am. Chem. Soc.* **2010**, *132*, 2160. (d) Sagara, Y.; Kato, T. *Angew. Chem. Int. Ed.* **2011**, *50*, 9128.
- (3) (a) Lee, Y.-A.; Eisenberg, R. *J. Am. Chem. Soc.* **2003**, *125*, 7778. (b) Ito, H.; Saito, T.; Oshima, N.; Kitamura, N.; Ishizaka, S.; Hinatsu, Y.; Wakeshima, M.; Kato, M.; Tsuge, K.; Sawamura, M. *J. Am. Chem. Soc.* **2008**, *130*, 10044. (c) Kozhevnikov, V. N.; Donnio, B.; Bruce, D. W. *Angew. Chem., Int. Ed.* **2008**, *47*, 6286. (d) Laguna, A.; Lasanta, T.; López-de-Luzuriaga, J. M.; Monge, M.; Naumov, P.; Olmos, M. E. *J. Am. Chem. Soc.* **2010**, *132*, 456. (e) Perruchas, S.; Goff, X. F. L.; Maron, L.; Maurin, I.; Guillen, F.; Gracia, A.; Gacoin, T.; Boilot, J.-P. *J. Am. Chem. Soc.* **2010**, *132*, 10967.
- (4) (a) Crenshaw, B. R.; Weder, C. *Chem. Mater.* **2003**, *15*, 4717. (b) Kunzelman, J.; Kinami, M.; Crenshaw, B. R.; Protasiewicz, J. D.; Weder, C. *Adv. Mater.* **2008**, *20*, 119. (c) Davis, D. A.; Hamilton, A.; Yang, J.; Cremer, L. D.; Gough, D. V.; Potisek, S. L.; Ong, M. T.; Braun, P. V.; Martínez, T. J.; White, S. R.; Moore, J. S.; Sottos, N. R. *Nature* **2009**, *459*, 68.
- (5) (a) Gentili, P. L.; Nocchetti, M.; Miliani, C.; Favaro, G. *New J. Chem.* **2004**, *28*, 379. (b) Dong, Y.; Xu, B.; Zhang, J.; Tan, X.; Wang, L.; Chen, J.; Lv, H.; Wen, S.; Li, B.; Ye, L.; Zou, B.; Tian, W. *Angew. Chem., Int. Ed.* **2012**, *51*, 10782.

(6) (a) Cozzolino, A. F.; Vargas-Baca, I.; Mansour, S.; Mahmoudkhani, A. H. *J. Am. Chem. Soc.* **2005**, *127*, 3184. (b) McEntee, G. J.; Vilela, F.; Skabara, P. J.; Anthopoulos, T. D.; Labram, J. G.; Tierney, S.; Harrington, R. W.; Clegg, W. *J. Mater. Chem.* **2011**, *21*, 2091.

(7) Concentrations of the CH<sub>2</sub>Cl<sub>2</sub> solutions were 2.5 × 10<sup>-5</sup> and 2.5 × 10<sup>-6</sup> M for the absorption and fluorescence measurements, respectively. Fluorescence quantum yield in CH<sub>2</sub>Cl<sub>2</sub> was 0.03.

(8) Recrystallization of the ground sample from CH<sub>2</sub>Cl<sub>2</sub> by slow evaporation produced the yellow-emissive crystals, while just annealing the ground sample did not lead to the recovery of the yellow-emissive state.

(9) Valeur, B.; Berberan-Santos, M. N. *Molecular Fluorescence*, 2nd ed.; Wiley-VCH: Weinheim, Germany, 2012.

(10) Winnik, F. M. *Chem. Rev.* **1993**, *93*, 587.

(11) Würthner, F.; Kaiser, T. E.; Saha-Möller, C. R. *Angew. Chem., Int. Ed.* **2011**, *50*, 3376.

(12) A small fluorescence band concomitantly increased at 460 nm may be attributed to a monomer emission observed from a partly disordered phase under high pressure.

(13) Yamamoto, T.; Sato, T.; Iijima, T.; Abe, M.; Fukumoto, H.; Koizumi, T.; Usui, M.; Nakamura, Y.; Yagi, T.; Tajima, H.; Okada, T.; Sasaki, Y.; Kishida, H.; Nakamura, A.; Fukuda, T.; Emoto, A.; Ushijima, H.; Kurosaki, C.; Hirota, H. *Bull. Chem. Soc. Jpn.* **2009**, *82*, 896.

(14) Crystallographic data for **1** at 296 K. (a) At the ambient pressure: monoclinic,  $P2_1/n$ ,  $a = 11.4016(5)$ ,  $b = 12.0000(4)$ ,  $c = 12.8329(5)$ ,  $\beta = 93.455(7)$ ,  $V = 1752.59(11)$  Å<sup>3</sup>,  $D_{\text{calcd}} = 1.579$  g·cm<sup>-3</sup>,  $Z = 4$ ,  $R_1 = 0.0442$  [ $I > 2.0\sigma(I)$ ],  $wR_2 = 0.1202$  (all data), GOF = 1.023 [ $I > 2.0\sigma(I)$ ]. (b) At 2.8 GPa: monoclinic,  $P2_1/n$ ,  $a = 11.182(7)$ ,  $b = 11.741(8)$ ,  $c = 11.941(7)$ ,  $\beta = 95.487(11)$ ,  $V = 1560.5(17)$  Å<sup>3</sup>,  $D_{\text{calcd}} = 1.773$  g·cm<sup>-3</sup>,  $Z = 4$ ,  $R_1 = 0.1195$  [ $I > 2.0\sigma(I)$ ],  $wR_2 = 0.2798$  (all data), GOF = 0.847 [ $I > 2.0\sigma(I)$ ].